ELSEVIER

Journal of Chromatography A, 930 (2001) 61–71

JOURNAL OF CHROMATOGRAPHY A

www.elsevier.com/locate/chroma

Investigation and interpretation of band broadening in size exclusion chromatography

J.P. Busnel[a,*], F. Foucault[a], L. Denis[a], W. Lee[b], T. Chang[b]

[a]*Faculté des Sciences, Université du Maine, 72085 Le Mans Cedex 9, France*

[b]*Department of Chemistry, POSTECH, Pohang 790-784, South Korea*

Received 29 May 2001; received in revised form 24 July 2001; accepted 24 July 2001

Abstract

Study of Band Broadening occurring in Size Exclusion Chromatography (SEC) is reported using very narrow PS standards obtained and characterised by Temperature Gradient Interaction Chromatography (TGIC). Chromatograms are fitted by Exponentially Modified Gaussian functions (EMG) and mapping of band broadening is obtained for different column sets. Interpretation of the skewing of the chromatograms is proposed with a new model using Brownian motion properties inside the pores. That explains why band broadening and tailing become so important near total exclusion volume.

Keywords: Band broadening; Temperature-gradient interaction chromatography; Peak shape; Exponentially modified Gaussian functions

1. Introduction

Size Exclusion Chromatography (SEC) is the most efficient technique to characterise MWD in soluble polymers. Since its introduction in 1964 by J.C. Moore [1], a large number of improvements have rendered the method more and more powerful.

Until 1975, a number of procedures concerning Band Broadening Correction (BBC) have been proposed to compensate the limited resolution of columns. The general problem has been presented by Tung [2] considering the spreading function as Gaussian.

In the simplest situation, the standard deviation of the spreading function σ is considered constant and the calibration curve is linear with a constant slope s: $\log(M) = a - s \cdot V_e$, V_e being the elution volume of species M at peak top. In that case, correction only depends on the dimensionless efficiency parameter σs, and for any chromatogram [3,4]:

$$M_{n_{corrected}} = M_{n_{uncorrected}} \exp(\sigma^2 s^2/2).$$
$$M_{w_{corrected}} = M_{w_{uncorrected}} \exp(-\sigma^2 s^2/2).$$

More thoroughly, a number of results have indicated that spreading increases with molecular mass and that skewing tends to appear for high molecular

*Corresponding author. Fax: +33-024-383-3315.

E-mail address: jean-pierre.busnel@univ-lemans.fr (J.P. Busnel).

0021-9673/01/$ – see front matter
PII: S0021-9673(01)01159-1

weights [5,6] but these indications were obscured by several practical limitations:

- Due to the limited sensitivity of detectors, it was very difficult to analyse high molecular mass samples at a sufficiently diluted concentration and often there were superposition of concentration effect and band broadening effect [7].
- There were difficulties to define precisely the polymolecularity of the standards used and peak shape was the combination of polymolecularity and band broadening [8].

Nevertheless methods have been proposed to take into account such non-uniform band broadening effect [9].

After 1975, a spectacular increase in column resolution rendered the problem of BBC less important, for simple detection it was generally possible to use columns for which no correction was needed.

More recently, there is a growing interest on BBC for several reasons:

- When analysing very high MW polymers, resolution is limited even with modern columns.
- Multiple detection techniques are very sensitive to imperfect resolution.
- As results become more and more reproducible, even small corrections become significant and useful.
- Modern computation facilities allow to routinely use complex mathematical correction methods.

In this work, we intend to take into account a major fact that is established when using modern columns: the peak of a uniform sample (pure species, perfectly isomolecular) is not Gaussian but skewed.

To produce information on the peak shape, it is essential to analyse very narrow standards and to determine their polymolecularity index independently of SEC. To this effect, we have used Temperature Gradient Interaction Chromatography (TGIC) [10–13] which exhibits higher resolution than SEC for analysing and fractionating PS standards. Excellent fits for the chromatograms of very narrow standards are obtained by using Exponentially Modified Gaussian functions (EMG) [14]. That allows a convenient mapping of the spreading characteristics of any chromatographic system. In the discussion we develop some theoretical arguments to interpret the different processes of BB in relation with the experimental results.

2. Experimental

2.1. Production of the ultra narrow PS samples

The list and some characteristics of the PS samples used in this work are given in Table 1.

The TGIC apparatus was described previously in detail [12]. An HPLC apparatus with a single C_{18} bonded silica column (Altech, Nucleosil, 100 Å pore, 4.6×250 mm, 5 μm particle size) was used with a UV/Vis absorption detector (LDC, Spectro Monitor 3000) operated at the wavelength of 260 nm. A low angle laser light scattering detector (LDC, KMX-6) was also used for the absolute molecular mass determination. The mobile phase was either a mixture of CH_2Cl_2/CH_3CN or tetrahydrofuran (THF)/methanol depending on the samples. All the solvents were used as received from Aldrich (HPLC grade). The eluent mixtures were pre-mixed and delivered by an isocratic pump (LDC, Constametric 3200) at a flow-rate of 0.5 ml/min. All samples were dissolved in a small portion of the eluent and injected via a Rheodyne 7125 injector equipped with a 20 μl sample loop. The column temperature was controlled in a pre-programmed manner by circulating a fluid from a bath/circulator (Neslab, RTE-111) through a home made column jacket.

Method 1. TGIC analysis with a light scattering detector was performed to determine the peak molecular mass (M_p) of a set of PS standards. Mobile phase was CH_2Cl_2/CH_3CN at 57/43 (v/v). Temperature was programmed from 20 to 40°C with optimised multiple steps gradient. In the calculation of M_p, a correction factor of 9% was considered to correct for preferential sorption (10). A 4th order polynomial calibration curve (log M vs. V_e) was obtained from the M_p values. The polymolecularity index $I_p = M_w/M_n$ was calculated according to the calibration curve.

Method 2. TGIC fractionation and characterisation of medium molecular mass PS.

Using the same experimental set up as in Method 1, temperature program was set to make the full width at half maximum of the elution peak around 5 min for the three PS's to be fractionated. Then a

Table 1
PS standards used in that study

Origin	Method	Nominal MW (g/mole)	$I_p = M_w/M_n$	Injected conc. (mg/cm^3)
Fract. by TGIC	3	578	1[a]	0.5
Fract. by TGIC	3	786	1[a]	0.5
Fract. by TGIC	3	994	1[a]	0.5
Fract. by TGIC	3	1250	1.006	0.5
Fract. by SEC	4	1800	1.009	0.5
Fract. by TGIC	3	3200	1.008	0.5
Fract. by TGIC	2	6200	1.009	0.5
Fract. by TGIC	2	15 300	1.002	0.5
Pressure Chemicals	1	33 000	1.004	0.5
Fract. by TGIC	2	68 500	1.003	0.5
Waters Ass.	4	98 000	1.007	0.5
Home made	1	113 000	1.006	0.5
Home made	1	135 000	1.005	0.5
Pressure Chemicals	1	200 000	1.004	0.5
Waters Ass.	1	384 000	1.004	0.5
Waters Ass.	4	470 000	1.011	0.5
Home made	1	648 000	1.006	0.4
Polymer Lab.	1	848 000	1.006	0.2
Waters Ass.	4	1 200 000	1.008	0.2
Home made	1	1 470 000	1.005	0.2
Fract by SEC	4	2 140 000	1.010	0.15
Fract by SEC	4	4 480 000	1.03	0.15
Fract by SEC	4	8 420 000	1.05	0.15

[a] Considered as pure oligomer.

fraction was collected for 2 min at the peak maximum position for each PS sample during the TGIC run. Collected fractions were dried under vacuum and redissolved to an appropriate concentration with the eluent for TGIC run to measure the molecular mass distribution of the fractions. TGIC chromatograms of five PS's (Mother PS's of three fractionated samples, PS 2450 and PS 113 000) were used to obtain a calibration curve and calculate I_p.

Method 3. TGIC fractionation of low molecular mass PS.

A mixed eluent of CH_2Cl_2/CH_3CN of 50/50 (v/v) was used as the mobile phase and the column temperature was 5°C for the fractionation of PS 3200 (Polymer lab., batch number 20126-6) and PS 1250 (Polymer Lab., batch number 20124-4). For the fractionation of the two low molecular mass samples, chromatographic separation was done under isothermal conditions. For PS 3200, 3 mg were injected and, 20 min after the injection, two eluate fractions were collected for 2 min each. For PS 1250, 3 mg was injected and, 9.5 min after the injection, three fractions of eluate were collected for 20 s each. As previously reported [10] a poorer eluent system was needed to fractionate PS 780 (Waters, Lot No. TN4166). For this fractionation, a mixed eluent of THF/methanol of 10/90 (v/v) was used. Column temperature was varied from 30 to 50°C during the chromatographic run. PS (3 mg) was injected and fully separated oligomer peaks were collected. The purity and molar mass of the first peaks of the series have been checked by LC–MS and GC–MS, giving molar masses equal to $58+104\times n$ as expected for PS *n*-mers obtained by butyl lithium initiator.

Method 4. SEC fractionation. Fractions are obtained by injecting, in normal running conditions, a commercial PS standard or a home made anionic PS, then collecting the central part of the peak (0.5 cm^3). The sample PS 1800 was fractionated on a column set PL gel 100 Å, 5 μm, 2×60 cm; the high MW PS are fractionated on a column set PL gel mixed B, 10

μm, 2×60 cm). The fractions were then injected for further analysis without concentration nor dilution. I_p from SEC is calculated applying K_n and K_w correction factors as explained later in the text.

2.2. SEC measurements

The spreading function of three columns sets, corresponding to different MW ranges of fractionation were investigated: The columns were: Jordi DVB 10^3 Å, 5 μm, 50 cm length for low MW (normal operating range 500–5×10^4 g/mole), Polymer Lab. PL gel mixed C, 5 μm, 60 cm length for medium MW (normal operating range 10^3–10^6 g/mole), two Polymer Lab. PL gel mixed B, 10 μm, 2×60 cm length for high MW (normal operating range 10^3–10^7 g/mole). The SEC apparatus consists in a constant flow pump, type P100 from Thermo Sep. Products, an automatic injector, type 234 from Gilson, a UV detector operating at 254 nm, type UV 1000 from Spectra Physics and a DR detector, type R410 from Waters. The eluent was THF at ambient temperature. Care was taken to prevent any column overloading, by checking that results were not dependant on injected volume and concentration. Concentration was reduced especially in the case of high MW standards. A proper design of filters and column fitting and reduced flow-rates were chosen to prevent mechanical degradation of the very high MW standards. For experiments concerning relaxation time (extra column effects), the injector was replaced by a six ports valve fitted with a 3 cm^3 loop; the column was replaced by a tubing of 0.7 mm I.D. and various lengths.

2.3. Chromatogram fits

For all SEC measurements, a home made software allowed data acquisition and treatment. Data files were then exported to the software PeakFit V04 from Jandel to check for the best adjustment. It appears that Exponentially Modified Gaussian functions (EMG) provide the best results, with correlation coefficients generally better than 0.999. EMG functions result from the convolution of a Gaussian function (standard deviation σ) with an exponential decay function (relaxation parameter τ). Such fits allows to define the spreading function for each standard peak with two parameters σ and τ [15].

Table 2
Mapping of band broadening parameters for column set Jordi gel 1000 Å, 50 cm

PS sample MW	V_{peak} (cm^3)	σ (cm^3)	τ (cm^3)	r^2
1 470 000	12.49	0.087	0.247	0.9989
384 000	13.37	0.077	0.191	0.9989
113 000	13.76	0.076	0.210	0.9992
98 000	13.95	0.072	0.194	0.9987
68 500	14.00	0.074	0.165	0.9994
33 000	14.81	0.139	0.163	0.9998
15 300	16.00	0.141	0.155	0.9995
6200	17.42	0.164	0.156	0.9998
3200	19.06	0.140	0.121	0.9999
1800	20.29	0.172	0.119	0.9997
1250	21.28	0.142	0.131	0.9996
994	21.74	0.122	0.123	0.9998
786	22.21	0.125	0.120	0.9996
578	22.79	0.115	0.110	0.9996

3. Results

Tables 2–4 present the results of the three column sets operated in the more classical running con-

Table 3
Mapping of band broadening parameters for column set PL gel mixed C, 60 cm

PS sample MW	V_{peak} (cm^3)	σ (cm^3)	τ (cm^3)	r^2
1 470 000	10.41	0.133	0.437	0.9999
848 000	10.96	0.142	0.178	0.9999
648 000	11.27	0.144	0.158	0.9995
470 000	11.72	0.136	0.142	0.9989
384 000	11.78	0.146	0.124	0.9990
200 000	12.41	0.138	0.127	0.9987
135 000	12.82	0.134	0.136	0.9992
113 000	12.99	0.141	0.135	0.9993
68 500	13.47	0.114	0.139	0.9997
33 000	14.37	0.140	0.126	0.9999
15 300	15.11	0.124	0.149	0.9998
6200	15.99	0.132	0.134	0.9997
3200	16.70	0.126	0.111	0.9997
1800	17.47	0.123	0.123	0.9990
1250	17.70	0.136	0.088	0.9998
578	18.36	0.113	0.083	0.9997

Table 4
Mapping of band broadening parameters for column set PL gel mixed B, 2×60 cm

PS sample MW	V_{peak} (cm^3)	σ (cm^3)	τ (cm^3)	r^2
8 420 000	19.25	0.160	0.380	0.9961
4 480 000	19.91	0.163	0.400	0.9918
2 150 000	21.12	0.240	0.402	0.9922
1 470 000	21.19	0.258	0.396	0.9974
848 000	22.10	0.248	0.268	0.9996
648 000	22.68	0.312	0.231	0.9917
384 000	23.81	0.288	0.210	0.9922
200 000	24.82	0.243	0.212	0.9977
135 000	25.50	0.244	0.211	0.9975
113 000	25.75	0.256	0.211	0.9971
33 000	27.97	0.229	0.197	0.9999

ditions. Systematic adjustment of experimental chromatogram with an EMG function was done using PeakFit V04 software. As shown in Fig. 1, quality of fit is generally excellent with correlation coefficients better than 0.999. Some distortions appear only when the high molecular mass samples are totally excluded from the column.

The presented results correspond to the Differential refractometer detector, that was systematically used independently of the nature of the sample. The refractometer design was changed by removing the major part of the entrance tubing. With this modification, the spreading between the two detectors was

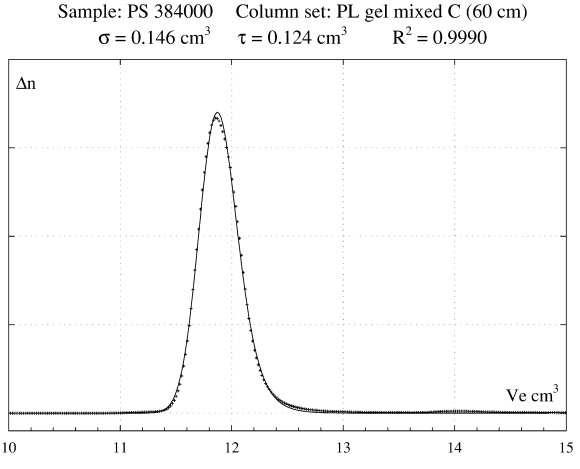

Fig. 1. Example of EMG fit for a very narrow PS standard: (continuous line for experimental data).

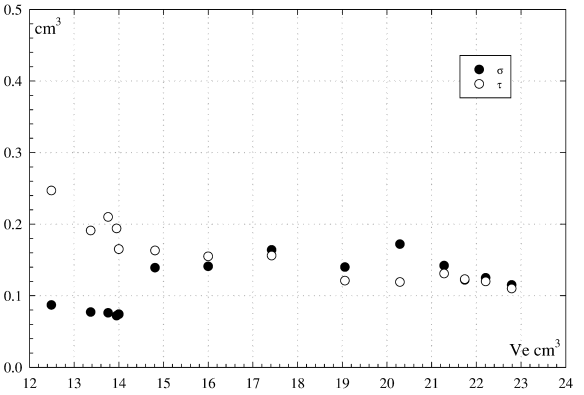

Fig. 2. Mapping of band broadening parameters for column set Jordi gel 1000 Å (50 cm) (*x* axis: elution volume; *y* axis: standard deviation σ and relaxation parameter τ, defining the best EMG fit for a set of very narrow PS standards).

minimised and the UV detector result was very close to that of the refractometer, with the values of σ and τ only a few percent lower.

Figs. 2–4, allow a rapid survey of the results. Even if there is some scattering on the results, this mapping of elementary peak shape is an efficient starting point for a rigorous BBC. Values of σ and τ versus elution volume can be fitted by a proper function (polynomial or other) and the exact shape of any elementary peak is then defined allowing convenient mathematical treatment of the problem.

Qualitatively, it appears that only limited changes

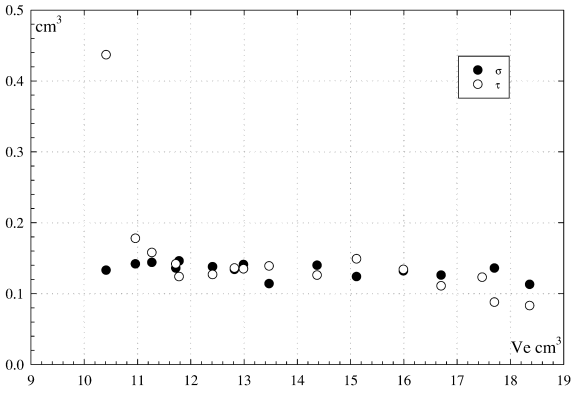

Fig. 3. Mapping of band broadening parameters for column set PL gel mixed C (60 cm) (*x* axis: elution volume; *y* axis: standard deviation σ and relaxation parameter τ, defining the best EMG fit for a set of very narrow PS standards).

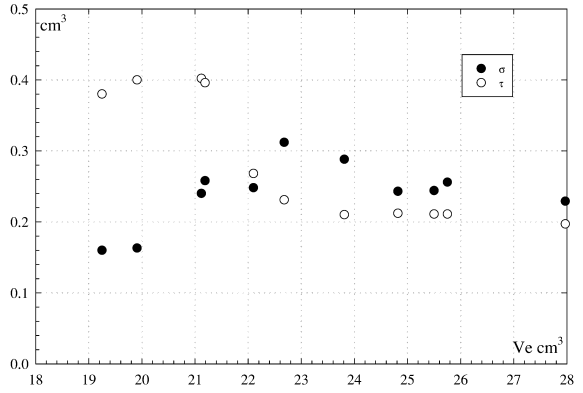

Fig. 4. Mapping of band broadening parameters for column set PL gel mixed B (2×60 cm) (*x* axis: elution volume; *y* axis: standard deviation σ and relaxation parameter τ, defining the best EMG fit for a set of very narrow PS standards).

on σ and τ are observed for samples which are totally eluted well after void volume. Dramatic changes appear only near total exclusion. For that reason, we propose a very simple correction method which can be useful for polydisperse samples, as long as they are eluted well inside the normal operating range of the column set.

We can consider as a first approximation that:

- peak shape is constant (i.e. for any isomolecular solute the peaks can be superposed by translation on the V_e axis and dilation on the *y* axis). One peak is defined by a set of h_i values equidistant on elution volume axis
- calibration curve is linear: $\log(M_i) = a - s \cdot V_i$ (V_i being the elution volume of species M_i at peak top).

From the chromatogram of an ideal isomolecular sample (practically a very narrow standard) we obtain the following uncorrected average molecular weights:

$$M_{n_{uncorrected}} = \Sigma\, h_i / \Sigma\, (h_i / M_i)$$
$$M_{w_{uncorrected}} = \Sigma\, (h_i M_i) / \Sigma\, h_i$$

since the real molecular mass is formally the molecular mass at peak top M_{peak} we define two correction factors to correct M_n and M_w:

$$K_n = M_{peak} / M_{n_{uncorrected}} \text{ and } K_w = M_{peak} / M_{w_{uncorrected}}$$

Any other narrow standard simply involves a shift along elution volume. We can run the same calculations: each M_i value is multiplied by a constant factor and M_{peak} is multiplied by the same factor. Thus the correction factors K_n and K_w are constants that define the system spreading function.

Table 5
Correction factors for band broadening

Column set	$K_n = M_{Peak} / M_{n_{uncorrected}}$	$K_w = M_{Peak} / M_{w_{uncorrected}}$
Jordi gel 1000 Å	1.030	1.025
PL gel mixed C	1.045	1.030
PL gel mixed B	1.070	1.030

Any wide chromatogram from polydisperse sample, obtained on the same system, is the addition of a set of isomolecular chromatograms. Thus, whatever is its shape, there is factorisation of the correction factors and:

$$M_{n_{corrected}} = K_n \cdot M_{n_{uncorrected}}$$
$$M_{w_{corrected}} = K_w \cdot M_{w_{uncorrected}}$$

Table 5 reports the correction factors for our three column sets in the classical running conditions. As standards are not strictly isomolecular, corrections are slightly overestimated. That confirms there is only minor average molecular mass corrections due to band broadening when using well adapted column sets.

4. Discussion

For the very narrow PS standards studied, with polymolecularity indexes lower than 1.01, we can consider that the molecular mass distribution effect is negligible. Contributions to band broadening are conveniently classified in: extra column effects, eddy dispersion, static dispersion, mass transfer.

In the classical chromatographic interpretation, each contribution is Gaussian, so there is simply addition of variances and we can define the number of theoretical plates $N = (V_e/\sigma)^2$ and use the so-called Van Deemter equation:

$$H = L/N = a + b/v + c \cdot v$$

(v: linear velocity of the eluent)

This classical interpretation is not sufficient, since

experimental results clearly indicate that there is peak skewing. Thus it is useful to study each contribution separately.

Extra column effects: (from capillary tubing, junctions, column end fittings, detector cells . . .):

It is difficult to study separately each of these categories however, it is easy to vary the contribution of the capillary tubing by using a chromatographic apparatus in which column is replaced by tubing of various lengths. When small volumes are injected into such a system, it is difficult to adjust the shape of the recorded signal, since it is highly dependent on the injection device characteristics. We have obtained better results injecting large volumes (3 cm^3), sufficient to obtain stationary situation in the detector, then observing the relaxation part of the signal after the end of the injection. We found that relaxation is correctly fitted by an exponential decay. It depends, not only on the geometry but also on the nature of the solute. As shown in Table 6, the relaxation volume strongly increases for high molecular mass solutes. To explain this, we note that in the usual situation the diffusion coefficient D of the solute is high enough to allow for a rapid averaging of radial positions. In that case the average velocity does not depend on the entrance position of the solute and the band broadening contribution is simply a Gaussian process. On the contrary in the case of high molecular mass solute, the diffusion coefficient is small. Solutes molecules which enter near the centre of the tube stay in the high velocity zone and those which enter near the walls stay in low velocity zones and that introduces skewing. Using the basic relation for Brownian motion $\langle x^2 \rangle = 2\ D \cdot t$ we can deduce that complete averaging of radial positions needs a time of transfer trough the tube greater than r^2/D. For classical chromatographic apparatus solutes stay a few seconds in the capillary tubes, which is clearly insufficient for averaging positions of high MW solutes. (For example, for $r = 0.1$ mm and $D = 2 \times 10^{-5}$ mm^2/s, that corresponds to a MW around 10^5 g/mole, about 500 s are needed.

Table 6
Relaxation time (seconds) for different tube lengths and solutes of different MW

Tube length	35 cm	125 cm	250 cm
Toluene	16	17	18
PS 20 000	44	60	65
PS 4 M	65	105	140

Eddy dispersion: According to the literature, this contribution is roughly independent of flow-rate and MW. For well packed columns it is Gaussian and the corresponding plate height, H, is smaller than the beads diameter (5 or 10 μm in our columns). The corresponding standard deviation expressed in elution volume units is established from the classical relation:

$$N = L/H = (V_e/\sigma)^2.$$

The σ values estimated from that relation are from 30 to 50% of the measured σ values.

Static dispersion: This classical contribution is Gaussian and we simply consider that it corresponds to the diffusion along the column axis, due to Brownian motion during the time t_0 spent in the interstitial volume: $\sigma = (2Dt_0)^{1/2}$. To compare with the experimental results where the standard deviation is expressed in elution volume, it is necessary to multiply by the effective cross section of the column (interstitial volume divided by the total length).

Thus, we can explicitly calculate the static dispersion contribution knowing the relation between the MW and the diffusion coefficient D. It is significant for low MW samples (especially at low flow-rates) and it vanishes for high MW polymers (Table 7).

Mass transfer: Here we need a less classical interpretation. Theoretical plates model predicts a Gaussian contribution, while experimental evidence shows skewing, that becomes very important for molecules eluted near V_0. Here we propose a more precise model for the steric exclusion process. Consider that each molecule visits n_v pores, spending in each visit a given time t_v.

The average time may be obtain from:

$$\langle t \rangle = \langle t_0 \rangle + \langle n_v \rangle \cdot \langle t_v \rangle$$

Where: $\langle t_0 \rangle$ is the mean time spent in the interstitial volume

$\langle n_v \rangle$ is the average number of visited pores.

Assume that $\langle n_v \rangle$ has the same order of magnitude as the number of theoretical plates (10^4). We can also estimate the total number of pores along the column:

Table 7
Static dispersion contribution for column PL gel mixed C, efficient cross section: 0.17 cm^2, For PS in THF at 20°C: $D = 3.4 \times 10^{-4}\ M^{0.564}$ (personal Ref.)

PS MW	D (cm^2/s)	σ (static contribution) cm^3	Relative static contribution
600	8.87E−06	0.0172	0.13
2000	4.47E−06	0.0122	0.10
6200	2.34E−06	0.0088	0.07
15 000	1.42E−06	0.0069	0.05
68 000	5.98E−07	0.0045	0.03
200 000	3.24E−07	0.0033	0.02

assuming that the pore radius is around 50 nm and L, the column length is around 50 cm, then $L/R_p = 10^7$. Thus the visit of a pore is a rare event (Poisson distribution) and the average number of visited pores $\langle n_v \rangle$ is proportional to the time spent in the interstitial volume.

Assume that $\langle t_v \rangle$ the average visit time is independent of the flow-rate since inside the pore, the liquid is stagnant. Consequently, the total time inside the pores ($\langle n_v \rangle \cdot \langle t_v \rangle$) is proportional to t_0 and we find again the classical observation that elution volume is independent of flow-rate.

Consider the parameters that govern $\langle n_v \rangle$:

From any position in the interstitial volume, the probability of reaching a pore entrance in a given time is proportional to D.

The time allowed to reach a pore entrance is inversely proportional to the linear velocity v.

Once at the pore entrance, the probability of being captured by the pore depends on the relative sizes of pore entrance and of solutes, so it is proportional to the classical partition coefficient K used in SEC.

Finally $\langle n_v \rangle \sim D \cdot v^{-1} \cdot K$

4.1. Discussion on $\langle t_v \rangle$

We consider that the distribution of t_v is governed by the properties of the solute Brownian motion. A simple representation is obtained considering pores as cylinders and studying a one dimension process along the cylinder axis, x being the abscissa and L the pore depth. As a first approach, we have run Monte Carlo simulations operating discrete jumps ± 1 for each unit of time. At time 0, $x = 0$, then at time $t+1$, $x = x + 1$ or $x = x - 1$ at random. The end of the visit corresponds either to $x < 0$ or $x > 2L$ (as the bottom of the pore can be considered as a virtual plane, the virtual outlet being at abscissa $2L$). In that condition $\langle t_v \rangle = 2L$ and we obtain a very highly skewed distribution of t_v. We have then simulated the situation for n independent visits and progressively we observe that the distribution of 't_v' comes back to a Gaussian one.

A more complete representation of the same model is obtained using the mathematical representation of a one-dimension Brownian motion. The molecule trajectory is modelled by a one-dimension Brownian motion starting from 0. Mathematically, this is a stochastic process $(B_t)_{t \geq 0}$ such that $B_0 = 0$, where is the time and for all t, B_t is a Gaussian variable with mean 0 and variance t, considering for simplicity of expressions that the diffusion coefficient $D = 1$.

We consider that the visit of a pore corresponds to the time spent by a Brownian motion between $-b$ and a where $a > 0$ and $b > 0$. Mathematically, this is the exit time of $[-b, a]$ by the Brownian motion, that we denote by the random variable $T_{b,a}$ and is given by the formula:

$$T_{b,a} = \inf\{t > 0, B_t > a \text{ or } B_t < -b$$

One can prove [16,17] that its law admits a density, f, and that the Laplace transform of f is given by:

$$\forall p > 0, L(f)(p) = E(e^{-pT_{b,a}}) = \frac{\cosh\left((a-b)\frac{\sqrt{p}}{\sqrt{2}}\right)}{\cosh\left((a+b)\frac{\sqrt{p}}{\sqrt{2}}\right)}$$

Here, we denote by E the expectation.

The explicit formula for f is much more complicated, it is given by:

$$\forall t >, f(t) = \frac{1}{\sqrt{2\pi t^3}} \sum_{n=-\infty}^{n=+\infty} \left[(2nL + b) \exp\left(-\frac{(2nL + b)^2}{2t} \right) + (2nL + a) \exp\left(-\frac{(2nL + a)^2}{2t} \right) \right]$$

where: $L = a + b$.

From this, we conclude that: $E(T_{b,a}) = ab$.

Thus, it is necessary to use a length b which corresponds to a capture length of the molecule by the pore and which can be roughly estimated as the molecule radius.

In a more general way, the Laplace transform of f permits us to calculate the moments of any order of $T_{b,a}$. For this, we expand $L(f)$ in integer series, as follows:

$$\begin{aligned} L(f)(p) &= E(\mathrm{e}^{-pT_{b,a}}) \\ &= E\left(1 - pT_{b,a} + \frac{p^2}{2} T_{b,a}^2 - \frac{p^3}{6} T_{b,a}^3 + \dots\right) \\ &= 1 - pE(T_{b,a}) + \frac{p^2}{2} E(T_{b,a}^2) - \frac{p^3}{6} E(T_{b,a}^3) + \dots \end{aligned}$$

identifying the terms, we can calculate the moments of $T_{b,a}$ and the various parameters defining the shape of the distribution: the relative standard deviation $\sigma/E(T)$ and the Fisher asymmetry parameter $\gamma_1 = E\{(T - E(T))^3\}/\sigma^3$ (see Table 8).

4.2. Case of a random number of visits

We now assume that the molecule visits N pores of the same length, where N is a random variable whose law is the Poisson distribution with mean $E(N) = n$. We denote by $T_{b,a}^i$ the time of visit of the ith pores and we assume that the times $T_{b,a}^i$ are independent.

Table 8
Moments and shape parameters of $T_{b,a}$: visit of one pore, various a/b values

a/b	$E(T_{b,a})$	$E(T_{b,a}^2)$	$E(T_{b,a}^3)$	$\sigma/E(T_{b,a})$	γ_1
1	1	1.67	4.06	0.82	1.96
4	1	2.42	9.13	1.19	2.30
9	1	4.04	26.98	1.74	3.19
16	1	6.35	68.93	2.31	4.19

The total time spent by the molecule in the pores is given by:

$$T = \sum_{i=1}^{N} T_{b,a}^i.$$

We can now prove that the law of T admits a density, g, and that the Laplace transform of g is given by:

$$\begin{aligned} \forall p > 0, L(g) &= E(\mathrm{e}^{-pT}) \\ &= E\left(\sum_{k=0}^{+\infty} 1_{\{N=k\}} \exp(-p \sum_{i=1}^{k} T_{b,a}^i) \right) \\ &= \sum_{k=0}^{+\infty} P(N = k) E\left(\prod_{i=1}^{k} \exp(-pT_{b,a}^i) \right) \\ &= \sum_{k=0}^{+\infty} P(N = k)(L(f)(p))^k \\ &= \sum_{k=0}^{+\infty} \frac{\mathrm{e}^{-n} n^k}{k!} (L(f)(p))^k \\ &= \exp(n(L(f)(p) - 1)). \end{aligned}$$

As before, we can calculate the moments of T and the shape parameters of the distribution for different values of n and a/b (see Table 9).

Both, the relative standard deviation $\sigma/E(T)$ and the Fisher asymmetry coefficient vary as $n^{-1/2}$, (this property is general for any Poisson summation as it can be easily demonstrated). Thus, as the mean number of visited pores increases, the distribution becomes narrower but still with some asymmetry. Additionally the ratio between Fisher asymmetry coefficient and the relative standard deviation has a small dependence on the ratio a/b (depth of the pore/radius of the molecule). The values in Table 9 give that ratio $\sim (a/b)^{\mathbf{0.015}}$. These mathematical expressions give us detailed information on the contribution of mass transfer to band broadening and these results explain why peak asymmetry becomes so important near total exclusion volume when the number of visited pores becomes small.

5. Conclusion

A convenient way for obtaining accurate information on band broadening in SEC is to analyse very

Table 9
Moments and shape parameters of $T_{b,a}$: mean number of visited pores n, various a/b values

n	a/b	$E(T)$	$E(T^2)$	$E(T^3)$	$\sigma/E(T)$	γ_1
1	1	1	2.66	10.07	1.29	1.89
1	4	1	3.42	17.38	1.55	2.43
1	9	1	4.04	40.09	2.01	3.33
1	16	1	7.35	88.99	2.52	4.30
2	1	2	7.33	36.13	0.91	1.34
2	4	2	8.83	55.26	1.10	1.72
2	9	2	12.07	110.4	1.42	2.35
2	16	2	16.71	222.1	1.78	3.04
5	1	5	33.33	270.33	0.58	0.85
5	4	5	37.08	351.90	0.70	1.09
5	9	5	45.19	562.68	0.90	1.49
5	16	5	56.77	946.21	1.13	1.92
10	1	10	116.67	1540	0.41	0.60
10	4	10	124.16	1816	0.49	0.77
10	9	10	140.37	2480	0.64	1.05
10	16	10	163.54	3595	0.80	1.36
100	1	100	10 166	1.05×10^6	0.13	0.19
100	4	100	10 241	1.07×10^6	0.16	0.24
100	9	100	10 403	1.12×10^6	0.20	0.33
100	16	100	10 635	1.19×10^6	0.25	0.43
1000	1	1000	10^6	1.00×10^9	0.041	0.060
1000	4	1000	10^6	1.00×10^9	0.049	0.077
1000	9	1000	10^6	1.01×10^9	0.064	0.105
1000	16	1000	10^6	1.02×10^9	0.080	0.136

narrow PS standards obtained after fractionation by TGIC. In normal running conditions, such peaks are not Gaussian but skewed and they can be well fitted by EMG functions.

We have observed several causes for skewing. For polymers, and related to their low diffusion coefficients, there is a tailing effect associated to an incomplete averaging of radial positions during the time spent along the tubing and in junction zones. But the main effect is observed for samples eluted near the total exclusion volume. In that case, the number of visited pores becomes small and the width and asymmetry of the peak increase, reflecting the large skewness of the visit time distribution into one pore.

Thus, for real life samples, we think that it is possible to properly correct for band broadening as long as the complete sample is eluted well after void volume. But the situation becomes much more complex if part of the sample is totally excluded or very near total exclusion. In that case, the sample fraction which is eluted near the total exclusion exhibits very large peak tailing and pollutes the chromatogram even far from void volume. Band broadening effect becomes extremely high and no appropriate correction method can be found. In such cases, priority is to find a column set with larger pore size.

Acknowledgements

This work is supported by a grant from the Center for Integrated Molecular Systems. The authors wish to thank Dr. P. Gosselin for help in GC–MS and LC–MS measurements and G. Guevelou for technical expertise in SEC analysis.

References

[1] J.C. Moore, J. Polym. Sci. A-2 (1964) 835.
[2] L.H. Tung, J. Appl. Polym. Sci. 10 (1966) 375.
[3] S.T. Balke, A.E. Hamielec, J. Appl. Polym. Sci. 13 (1969) 1881.
[4] J.P. Busnel, C.M. Bruneau, Analysis 2 (1983) 72.

[5] A.C. Ouano, J.A. Biesenberger, J. Chromatogr. 55 (1971) 145.
[6] H.W. Osterhoudt, L.N. Ray, J. Polym. Sci. A2 (5) (1967) 569.
[7] J. Janca, Anal. Chem. 51 (1979) 637.
[8] J.V. Dawkins, G. Yeadon, J. Chromatogr. 206 (1981) 215.
[9] A.E. Hamielec, Correction for axial dispersion, in: J. Janca (Ed.), Steric Exclusion Liquid Chromatography of Polymers, Marcel Dekker, New York, 1984, p. 117.
[10] H.C. Lee, T. Chang, S. Harville, J.W. Mays, Macromolecules 31 (1998) 690.
[11] W. Lee, H. Lee, J. Cha, T. Chang, K.J. Hanley, T.P. Lodge, Macromolecules 33 (2000) 511.
[12] T. Chang, H.C. Lee, W. Lee, S. Park, C. Ko, Macromol. Chem. Phys. 200 (1999) 2188.
[13] W. Lee, H.C. Lee, T. Park, T. Chang, J.Y. Chang, Polymer 40 (1999) 7227.
[14] E. Grushka, Anal. Chem. 44 (1972) 1733.
[15] F. Foucault, Ph.D. Thesis, University of Paris VI, 1998.
[16] I. Karatzas, S. Shreve, Brownian Motion and Stochastic Calculus, Springer-Verlag, New York, 1988.
[17] D. Revuz, M. Yor, Continuous Martingales and Brownian Motion, Chapter II, Springer-Verlag, New York, 1991.